

Ditelluroether Complexes of Manganese and Rhenium Carbonyl Halides: Synthesis and IR and Multinuclear NMR Spectroscopic and Structural Studies. Comparison of the Bonding Properties of Dithio-, Diseleno-, and Ditelluroethers in Low-Valent Carbonyl Systems

William Levason,* Simon D. Orchard, and Gillian Reid

Department of Chemistry, University of Southampton, Southampton SO17 1BJ, U.K.

Received October 19, 1998

The synthesis of the ditelluroether complexes of Mn(I) and Re(I) carbonyl halides [MnX(CO)₃(L-L)] (X = Cl, Br, I; L-L = MeTe(CH₂)₃TeMe, PhTe(CH₂)₃TePh, *o*-C₆H₄(TeMe)₂) and [ReX(CO)₃(L-L)] (X = Cl, Br) are described. The complexes have been characterized by analysis, IR and multinuclear NMR spectroscopy (¹H, ¹³C{¹H}, ⁵⁵Mn, ¹²⁵Te{¹H}), and FAB mass spectrometry. Crystal structures of [MCl(CO)₃{*o*-C₆H₄(TeMe)₂}] (M = Mn, Re) are also included and show the ditelluroether adopting the *meso*-2 arrangement with the complexes in a distorted six-coordinate geometry. [ReBr(CO)₃{*o*-C₆H₄(SeMe)₂}] and [MnCl(CO)₃L₂] (L = Me₂S, Me₂Se, Me₂Te) have also been prepared and spectroscopically characterized. Detailed comparisons of the spectroscopic data for these and analogous thio- and selenoether species are made. Specifically, comparison of the force constants of the C_s symmetry M(CO)₃ fragments and the relative magnitudes of δ(⁵⁵Mn) and the ¹²⁵Te:⁷⁷Se ratio of the chemical shifts of analogous compounds are interpreted in terms of the relative coordinating abilities of the group 16 donor bidentate ligands. On this basis the telluroether compounds show significantly enhanced σ-donation compared with the lighter analogues, consistent with theoretical predictions.

Introduction

In the 10 years since a range of chelating ditelluroether ligands was reported,¹ thorough investigations of their coordination chemistry with a variety of metals in medium oxidation states have been carried out: viz., palladium(II), platinum(II),² iridium(III),^{2,3} and cobalt(III) halides,⁴ homoleptic copper(I) and silver(I) systems,⁵ and tin(IV) halides.⁶ Quantitative studies of pyramidal inversion barriers in [PtMe₃I(ditelluroether)] have shown that the inversion barriers increase in the order S < Se < Te in comparable systems.⁷ In contrast to the dithio and diseleno analogues, ditelluroethers do not form stable compounds with high-valent platinum metal halides such as Pt(IV), Ir(IV), and Os(VI).⁸ Thus, a reasonable amount of data are available on which an assessment of the relative bonding properties of analo-

gous S, Se, and Te ligands toward positive-oxidation-state metals can be based.⁸ In marked contrast, the chemistry of these ligands with metal carbonyls is unexplored. Theoretical studies by Schumann and Hoffmann⁹ predict that in low-valent complexes such as those involving carbonyls, the M–L (L = S, Se, Te) bond strengths increase as group 16 is descended, and there is some evidence from the chemistry of R₂E ligands¹⁰ that this may be so. Here we report the synthesis and detailed spectroscopic studies of ditelluroether complexes with manganese and rhenium carbonyl halides of the type [MX(CO)₃(L-L)] and comparisons of their spectroscopic properties with those of dithioether and diselenoether analogues.^{11,12}

Results

Synthesis and Spectroscopic Characterization. The [Mn(CO)₃X(L-L)] (X = Cl, Br, I; L-L = MeTe(CH₂)₃-

(1) Hope, E. G.; Kemmitt, T.; Levason, W. *Organometallics* **1988**, *7*, 78. Kemmitt, T.; Levason, W. *Organometallics* **1989**, *8*, 1303.

(2) Kemmitt, T.; Levason, W.; Webster, M. *Inorg. Chem.* **1989**, *28*, 692. Kemmitt, T.; Levason, W. *Inorg. Chem.* **1990**, *29*, 731.

(3) Cipriano, R. A.; Hanton, L. R.; Levason, W.; Pletcher, D.; Powell, N. A.; Webster, M. *J. Chem. Soc., Dalton Trans.* **1988**, 2483.

(4) Brown, J. L.; Kemmitt, T.; Levason, W. *J. Chem. Soc., Dalton Trans.* **1990**, 1513.

(5) Black, J. R.; Champness, N. R.; Levason, W.; Reid, G. *J. Chem. Soc., Dalton Trans.* **1995**, 3439. Black, J. R.; Champness, N. R.; Levason, W.; Reid, G. *Inorg. Chem.* **1996**, *35*, 1820.

(6) Genge, A. R. J.; Levason, W.; Reid, G. *J. Chem. Soc., Dalton Trans.* **1997**, 4549.

(7) Abel, E. W.; Orrell, K. G.; Scanlan, S. P.; Stevenson, D.; Kemmitt, T.; Levason, W. *J. Chem. Soc., Dalton Trans.* **1991**, 591.

(8) For a review see: Hope, E. G.; Levason, W. *Coord. Chem. Rev.* **1993**, *122*, 109.

(9) Schumann, H.; Arif, A. A.; Rheingold, A. L.; Janiak, C.; Hoffmann, R.; Kuhn, N. *Inorg. Chem.* **1991**, *30*, 1618.

(10) Kuhn, H.; Schumann, H. *J. Organomet. Chem.* **1984**, *276*, 55. Kuhn, H.; Schumann, H.; Zauder, E. *J. Organomet. Chem.* **1987**, *327*, 17.

(11) Connolly, J.; Goodban, G. W.; Reid, G.; Slawin, A. M. Z. *J. Chem. Soc., Dalton Trans.* **1998**, 2225. Connolly, J.; Davies, M. K.; Reid, G. *J. Chem. Soc., Dalton Trans.* **1998**, 3833.

(12) Abel, E. W.; Bhargava, S. K.; Bhatti, M. M.; Kite, K.; Mazid, M. A.; Orrell, K. G.; Sik, V.; Williams, B. L.; Hursthouse, M. B.; Malik, K. M. A. *J. Chem. Soc., Dalton Trans.* **1982**, 2065. Abel, E. W.; Bhatti, M. M.; Orrell, K. G.; Sik, V. *J. Organomet. Chem.* **1981**, *208*, 195. Abel, E. W.; Bhargava, S. K.; Bhatti, M. M.; Mazid, M. A.; Orrell, K. G.; Sik, V.; Hursthouse, M. B.; Malik, K. M. A. *J. Organomet. Chem.* **1983**, *250*, 373.

Table 1. Selected ^{55}Mn , ^{77}Se , and ^{125}Te NMR Data

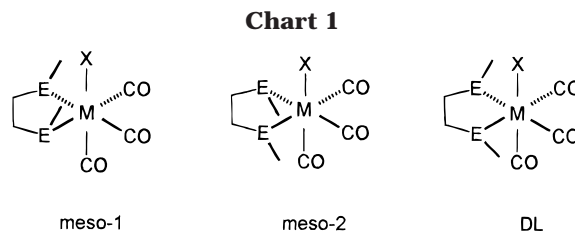
compd	$\delta(^{55}\text{Mn})^a$	$\delta(^{125}\text{Te}\{^1\text{H}\})^b$	<i>meso-2:DL:meso-1</i> ^c
[Mn(CO) ₃ Cl{ <i>o</i> -C ₆ H ₄ (TeMe) ₂ }]	-774 (3000), -717 (1500)	829, 824 (br)	1:1:0
[Mn(CO) ₃ Br{ <i>o</i> -C ₆ H ₄ (TeMe) ₂ }]	-901 (2800), -827 (1660)	818, 817, 815	10:1:0
[Mn(CO) ₃ I{ <i>o</i> -C ₆ H ₄ (TeMe) ₂ }]	-1146 (2800), -1050 (1200)	806, 786	10:1:0
[Mn(CO) ₃ Cl{MeTe(CH ₂) ₃ TeMe}]	-644 (2000), -594 (sh), -581 (1700)	280, 234, 203, 185	1:1.5:1
[Mn(CO) ₃ Br{MeTe(CH ₂) ₃ TeMe}]	-753 (1855), -690 (1640)	260, 213, 180, 165	1:0.8:0.5
[Mn(CO) ₃ I{MeTe(CH ₂) ₃ TeMe}]	-975 (1500), -916 (1500), -888 (sh)	226, 225, 206, 135	1:1:0.1
[Mn(CO) ₃ Cl{PhTe(CH ₂) ₃ TePh}]	-435, -500, -613	dec (see text)	
[Mn(CO) ₃ Br{PhTe(CH ₂) ₃ TePh}]	-634, -568	dec (see text)	
[Mn(CO) ₃ Cl(SMe ₂) ₂]	-57 (800)		
[Mn(CO) ₃ Cl(SeMe ₂) ₂]	-205 (2200)	66 ^d	
[Mn(CO) ₃ Cl(TeMe ₂) ₂]	-637 (1600), -920 (20 000) ^e	161, 271 ^e	
[Re(CO) ₃ Cl{ <i>o</i> -C ₆ H ₄ (TeMe) ₂ }]		629, 625, 612, 599.5	1:0.5:0.5
[Re(CO) ₃ Br{ <i>o</i> -C ₆ H ₄ (TeMe) ₂ }]		616, 606.5, 593.5	1:0.5:0
[Re(CO) ₃ Cl{MeTe(CH ₂) ₃ TeMe}]		101, 77, 20, 19.5	1:1:1
[Re(CO) ₃ Br{MeTe(CH ₂) ₃ TeMe}]		78, 57, -4.5, -6	1:2:1
[Re(CO) ₃ Br{ <i>o</i> -C ₆ H ₄ (SeMe) ₂ }]		305, 294, 289, 272 ^d	1:1:0.1

^a In CH₂Cl₂/CDCl₃ solution at 300 K, relative to external KMnO₄ in water; $w_{1/2}$ /Hz in parentheses. ^b Relative to neat external TeMe₂. ^c Approximate invertomer populations. ^d $^{77}\text{Se}\{^1\text{H}\}$ NMR relative to neat external SeMe₂. ^e Resonance of *mer,trans* isomer.

TeMe, *o*-C₆H₄(TeMe)₂, PhTe(CH₂)₃TePh were synthesized by the reaction of the ditelluroether ligand with the appropriate [Mn(CO)₅X] compound in a 1:1 molar ratio in chlorocarbon solvents. The corresponding rhenium complexes [Re(CO)₃X(L-L)] (X = Cl, Br; L-L = MeTe(CH₂)₃TeMe, *o*-C₆H₄(TeMe)₂) were made similarly from [Re(CO)₅X]. Monitoring the reactions by solution IR spectroscopy showed that the rates of reaction followed the usual sequence (Cl > Br > I; Mn > Re) and that no other products were formed. The reactions were conducted in vessels wrapped with aluminum foil to exclude light. The solid complexes of both metals with MeTe(CH₂)₃TeMe and *o*-C₆H₄(TeMe)₂ are air-stable but decompose slowly in solution, especially in the presence of oxygen or in bright light. In contrast, the manganese complexes of PhTe(CH₂)₃TePh, although reasonably stable as solids, decompose very rapidly in solution, even in the dark, and this limited the spectroscopic data obtainable (the Re analogues were not prepared). The limited range of ditelluroether ligands used reflects the fact that 1,2-di-R-telluroalkanes are unknown.¹ The three compounds [Mn(CO)₃Cl(EMe₂)₂] (E = S, Se, Te) and the two species [Re(CO)₃Br{*o*-C₆H₄(EMe₂)₂}] (E = S, Se) were made similarly for comparison.¹³

The identification of the products as *fac*-[M(CO)₃X(L-L)] (M = Mn, Re; Table 1) follows from elemental analysis, the FAB mass spectra, which show prominent [M(CO)₃X(L-L)]⁺, [MX(L-L)]⁺, and [M(CO)₃(L-L)]⁺ ions, and the IR spectra and was confirmed by X-ray crystallographic studies of two examples. The IR spectra exhibit three $\nu(\text{CO})$ modes both as CsI disks and in CHCl₃ solution (Table 2), consistent with the local C₃ symmetry present (theory 2A' + A'').

The coordinated ditelluroethers are chiral, producing the four diastereoisomers (invertomers) *meso-1*, *meso-2*, and a *DL* pair (Chart 1), which are expected to interconvert via pyramidal inversion at tellurium.⁷ The invertomers are readily identified by NMR spectroscopy (the *DL* pair are NMR indistinguishable, although due to the lack of a plane of symmetry each RTe- group of the *DL* form affords a separate resonance). In the present work we have recorded ^1H , $^{13}\text{C}\{^1\text{H}\}$, $^{125}\text{Te}\{^1\text{H}\}$, and ^{55}Mn NMR spectra. Pyramidal inversion barriers



increase in the order S < Se < Te,⁷ and in the present complexes inversion is slow on the time scales appropriate to each of the observed nuclei; hence, the resonances of the individual invertomers are observed (Table 1 and Supporting Information). The relative abundances of the invertomers vary widely in different systems and are a subtle reflection of both steric and electronic factors (when fewer than expected resonances are seen in a particular spectrum, this may reflect either low abundance of one form or, since the chemical shift differences are often small, accidental coincidence of resonances). For [Mn(CO)₃Cl{MeTe(CH₂)₃TeMe}], the ^1H and $^{13}\text{C}\{^1\text{H}\}$ NMR spectra each contain four $\delta(\text{Me})$ resonances, and there are four resonances in the $^{125}\text{Te}\{^1\text{H}\}$ spectra, consistent with the presence of significant amounts of all the invertomers: viz., *meso-1* (one resonance), *meso-2* (one resonance), and *DL* (two resonances). Due to the effect of the ^{55}Mn quadrupole ($Q = 0.55 \times 10^{-28} \text{ m}^2$) the $\delta(\text{CO})$ resonances are very broad in the $^{13}\text{C}\{^1\text{H}\}$ NMR spectrum, which also prevents useful comparison of these chemical shifts with those in complexes with other neutral ligands. Similar ^1H , $^{13}\text{C}\{^1\text{H}\}$, and $^{125}\text{Te}\{^1\text{H}\}$ NMR data were obtained for [Mn(CO)₃X{MeTe(CH₂)₃TeMe}] (X = Br, I) (Table 1). However, for [Mn(CO)₃X{*o*-C₆H₄(TeMe)₂}] (X = Cl, Br, I) the NMR spectra suggest that only two invertomers are present in substantial amounts, the three Me resonances in both the ^1H and $^{13}\text{C}\{^1\text{H}\}$ NMR spectra indicating that the *DL* and one *meso* form are present. Comparison with data on related systems suggest^{11,12} that the *meso-1* form, which often has destabilizing X··Me interactions, is likely to be the least populated invertomer. The coordination shifts ($\Delta = \delta_{\text{complex}} - \delta_{\text{free ligand}}$) in the $^{125}\text{Te}\{^1\text{H}\}$ NMR spectra (Table 4) show the usual dependence^{2,8} upon chelate ring size, being small for the six-membered rings in complexes of MeTe(CH₂)₃-TeMe and very large for the five-membered rings formed

(13) Belforte, A.; Calderazzo, F.; Vitali, D.; Zanazzi, P. F. *Gazz. Chim. Ital.* **1985**, *115*, 125.

Table 2. $[\text{M}(\text{CO})_3\text{X}(\text{L-L})]$ $\nu(\text{CO})$ Frequencies and Derived Force Constants

compd	$\nu(\text{CO})^a$			K_1^b	K_2^b	k_1^b
	A'(2)	A''	A'(1)			
$[\text{Mn}(\text{CO})_3\text{Cl}\{\text{o-C}_6\text{H}_4(\text{TeMe})_2\}]$	2026 (s)	1957 (m)	1916 (m)	15.07	15.90	0.43
$[\text{Mn}(\text{CO})_3\text{Br}\{\text{o-C}_6\text{H}_4(\text{TeMe})_2\}]$	2024 (s)	1956 (m)	1917 (m)	15.09	15.87	0.42
$[\text{Mn}(\text{CO})_3\text{I}\{\text{o-C}_6\text{H}_4(\text{TeMe})_2\}]$	2020 (s)	1954 (m)	1918 (m)	15.10	15.83	0.41
$[\text{Mn}(\text{CO})_3\text{Cl}\{\text{MeTe}(\text{CH}_2)_3\text{TeMe}\}]$	2021 (s)	1949 (m)	1906 (m)	14.93	15.79	0.45
$[\text{Mn}(\text{CO})_3\text{Br}\{\text{MeTe}(\text{CH}_2)_3\text{TeMe}\}]$	2019 (s)	1949 (m)	1907 (m)	14.94	15.78	0.46
$[\text{Mn}(\text{CO})_3\text{I}\{\text{MeTe}(\text{CH}_2)_3\text{TeMe}\}]$	2016 (s)	1947 (m)	1908 (m)	14.95	15.74	0.43
$[\text{Mn}(\text{CO})_3\text{Cl}\{\text{PhTe}(\text{CH}_2)_3\text{TePh}\}]$	2025 (s)	1957 (m)	1917 (m)	15.08	15.89	0.43
$[\text{Mn}(\text{CO})_3\text{Br}\{\text{PhTe}(\text{CH}_2)_3\text{TePh}\}]$	2024 (s)	1959 (m)	1914 (m)	15.02	15.91	0.42
$[\text{Mn}(\text{CO})_3\text{Cl}(\text{SMe}_2)_2]$	2034 (s)	1954 (s)	1920 (s)	15.20	15.91	0.49
$[\text{Mn}(\text{CO})_3\text{Cl}(\text{SeMe}_2)_2]$	2027 (s)	1948 (s)	1916 (s)	15.14	15.80	0.48
$[\text{Mn}(\text{CO})_3\text{Cl}(\text{TeMe}_2)_2]$	2017 (s)	1942 (m)	1907 (m)	14.97	15.69	0.46
$[\text{Mn}(\text{CO})_3\text{Cl}\{\text{o-C}_6\text{H}_4(\text{SeMe})_2\}]^c$	2037	1964	1924	15.22	16.03	0.46
$[\text{Mn}(\text{CO})_3\text{Br}\{\text{o-C}_6\text{H}_4(\text{SeMe})_2\}]^c$	2035	1963	1924	15.21	16.01	0.45
$[\text{Mn}(\text{CO})_3\text{I}\{\text{o-C}_6\text{H}_4(\text{SeMe})_2\}]^c$	2030	1960	1924	15.21	15.95	0.43
$[\text{Mn}(\text{CO})_3\text{Cl}\{\text{MeSe}(\text{CH}_2)_3\text{SeMe}\}]^c$	2032	1955	1917	15.13	15.91	0.47
$[\text{Mn}(\text{CO})_3\text{Br}\{\text{MeSe}(\text{CH}_2)_3\text{SeMe}\}]^c$	2030	1954	1918	15.15	15.88	0.47
$[\text{Mn}(\text{CO})_3\text{I}\{\text{MeSe}(\text{CH}_2)_3\text{SeMe}\}]^c$	2025	1951	1918	15.14	15.82	0.45
$[\text{Mn}(\text{CO})_3\text{Cl}\{\text{o-C}_6\text{H}_4(\text{SMe})_2\}]^c$	2041	1965	1927	15.28	16.06	0.47
$[\text{Mn}(\text{CO})_3\text{Br}\{\text{o-C}_6\text{H}_4(\text{SMe})_2\}]^c$	2039	1965	1927	15.27	16.05	0.46
$[\text{Mn}(\text{CO})_3\text{I}\{\text{o-C}_6\text{H}_4(\text{SMe})_2\}]^c$	2035	1963	1928	15.29	16.01	0.44
$[\text{Mn}(\text{CO})_3\text{Cl}\{\text{MeS}(\text{CH}_2)_3\text{SMe}\}]^c$	2036	1954	1923	15.27	15.91	0.50
$[\text{Mn}(\text{CO})_3\text{Br}\{\text{MeS}(\text{CH}_2)_3\text{SMe}\}]^c$	2034	1955	1924	15.27	15.91	0.48
$[\text{Mn}(\text{CO})_3\text{I}\{\text{MeS}(\text{CH}_2)_3\text{SMe}\}]^c$	2031	1957	1927	15.29	15.91	0.45
$[\text{Re}(\text{CO})_3\text{Cl}\{\text{o-C}_6\text{H}_4(\text{TeMe})_2\}]$	2032 (s)	1951 (m)	1908 (m)	15.00	15.87	0.50
$[\text{Re}(\text{CO})_3\text{Br}\{\text{o-C}_6\text{H}_4(\text{TeMe})_2\}]$	2031 (s)	1952 (m)	1908 (m)	14.99	15.88	0.50
$[\text{Re}(\text{CO})_3\text{Cl}\{\text{MeTe}(\text{CH}_2)_3\text{TeMe}\}]$	2028 (s)	1942 (m)	1899 (m)	14.89	15.76	0.53
$[\text{Re}(\text{CO})_3\text{Br}\{\text{MeTe}(\text{CH}_2)_3\text{TeMe}\}]$	2028 (s)	1943 (m)	1901 (m)	14.91	15.77	0.52
$[\text{Re}(\text{CO})_3\text{Br}\{\text{o-C}_6\text{H}_4(\text{SeMe})_2\}]$	2038 (s)	1953 (m)	1911 (m)	15.07	15.93	0.52
$[\text{Re}(\text{CO})_3\text{Cl}\{\text{MeSe}(\text{CH}_2)_3\text{SeMe}\}]^d$	2034	1938	1906	15.07	15.74	0.57
$[\text{Re}(\text{CO})_3\text{Br}\{\text{MeSe}(\text{CH}_2)_3\text{SeMe}\}]^d$	2038	1942	1906	15.06	15.81	0.58
$[\text{Re}(\text{CO})_3\text{I}\{\text{MeSe}(\text{CH}_2)_3\text{SeMe}\}]^d$	2036	1944	1906	15.03	15.82	0.56
$[\text{Re}(\text{CO})_3\text{Br}\{\text{o-C}_6\text{H}_4(\text{SMe})_2\}]$	2041 (s)	1957 (m)	1913 (m)	15.09	15.99	0.52
$[\text{Re}(\text{CO})_3\text{Cl}\{\text{MeS}(\text{CH}_2)_3\text{SMe}\}]^d$	2037	1945	1912	15.14	15.83	0.55
$[\text{Re}(\text{CO})_3\text{Br}\{\text{MeS}(\text{CH}_2)_3\text{SMe}\}]^d$	2042	1950	1914	15.16	15.91	0.56
$[\text{Re}(\text{CO})_3\text{I}\{\text{MeS}(\text{CH}_2)_3\text{SMe}\}]^d$	2038	1948	1912	15.12	15.87	0.55

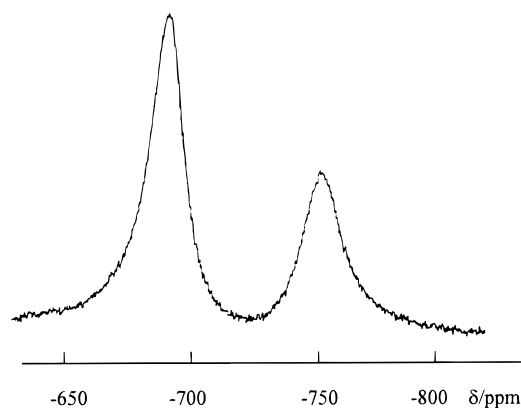
^a In CHCl_3 solution; in units of cm^{-1} . ^b In units of $\text{mdyn } \text{\AA}^{-1}$. ^c Frequency data from ref 11. ^d Frequency data from ref 12.

Table 3. Selected Bond Lengths and Angles for $[\text{Mn}(\text{CO})_3\text{Cl}\{\text{o-C}_6\text{H}_4(\text{TeMe})_2\}]$ and $[\text{Re}(\text{CO})_3\text{Cl}\{\text{o-C}_6\text{H}_4(\text{TeMe})_2\}]$

$[\text{Mn}(\text{CO})_3\text{Cl}\{\text{o-C}_6\text{H}_4(\text{TeMe})_2\}]$		$[\text{Re}(\text{CO})_3\text{Cl}\{\text{o-C}_6\text{H}_4(\text{TeMe})_2\}]$	
Bond Lengths (Å)			
Te(1)–Mn(1)	2.598(1)	Te(1)–Re(1)	2.7416(9)
Te(2)–Mn(1)	2.613(1)	Te(2)–Re(1)	2.729(1)
Mn(1)–Cl(1)	2.411(2)	Re(1)–Cl(1)	2.508(3)
Mn(1)–C(10)	1.819(9)	Re(1)–C(1)	1.93(1)
Mn(1)–C(9)	1.821(9)	Re(1)–C(2)	1.91(1)
Mn(1)–C(11)	1.791(9)	Re(1)–C(3)	1.91(1)
Bond Angles (deg)			
Te(1)–Mn(1)–Te(2)	87.60(4)	Te(1)–Re(1)–Te(2)	85.42(3)
Te(1)–Mn(1)–C(9)	173.9(3)	Te(1)–Re(1)–C(2)	178.7(3)
Te(1)–Mn(1)–C(11)	92.5(3)	Te(1)–Re(1)–C(1)	91.2(3)
Te(1)–Mn(1)–Cl(1)	83.23(6)	Te(1)–Re(1)–Cl(1)	87.33(7)
Te(1)–Mn(1)–C(10)	93.0(3)	Te(1)–Re(1)–C(3)	89.9(3)
Te(2)–Mn(1)–C(9)	88.9(3)	Te(2)–Re(1)–Cl(1)	82.47(7)
Te(2)–Mn(1)–Cl(1)	87.82(7)	Te(2)–Re(1)–C(1)	92.4(4)
Te(2)–Mn(1)–C(10)	179.2(3)	Te(2)–Re(1)–C(3)	174.1(3)
Te(2)–Mn(1)–C(11)	90.2(3)	Te(2)–Re(1)–C(2)	94.1(3)
Cl(1)–Mn(1)–C(9)	91.7(3)	Cl(1)–Re(1)–C(2)	93.8(3)
Cl(1)–Mn(1)–C(10)	91.7(3)	Cl(1)–Re(1)–C(3)	93.7(3)
Cl(1)–Mn(1)–C(11)	175.4(3)	Cl(1)–Re(1)–C(1)	174.8(4)
C(9)–Mn(1)–C(10)	90.5(4)	Cl(1)–Re(1)–C(2)	87.7(5)
C(9)–Mn(1)–C(11)	92.5(4)	C(1)–Re(1)–C(3)	91.3(5)
C(10)–Mn(1)–C(11)	90.3(4)	C(2)–Re(1)–C(3)	90.7(5)

by $\text{o-C}_6\text{H}_4(\text{TeMe})_2$; this is further confirmation that the ditelluroethers are chelating in all of the complexes.

For the $[\text{Mn}(\text{CO})_3\text{X}(\text{L-L})]$ complexes, it was also possible to record ^{55}Mn NMR spectra (Table 1; ^{55}Mn , $I = 5/2$, 100%, $\Xi = 24.64$ MHz, $D_c = 994$, $Q = 0.55 \times 10^{-28}$ m^2).¹⁴ The line width varies widely with the electric field

**Figure 1.** ^{55}Mn NMR spectrum of *fac*- $[\text{Mn}(\text{CO})_3\text{Br}\{\text{MeTe}(\text{CH}_2)_3\text{TeMe}\}]$.

gradient at the nucleus, and in the present manganese complexes, line widths were moderate (≤ 3000 Hz), allowing resonances of individual invertomers to be resolved (Table 1, Figure 1). Accumulation times are only a few minutes for moderately concentrated solutions, and even for the unstable $[\text{Mn}(\text{CO})_3\text{X}\{\text{PhTe}(\text{CH}_2)_3\text{TePh}\}]$ complexes, ^{55}Mn spectra were easily observed. The manganese chemical shift is a useful indicator of the donor set (see Figure 2).

The $[\text{Mn}(\text{CO})_3\text{Cl}(\text{EMe}_2)_2]$ complexes ($\text{E} = \text{S}, \text{Se}$) are readily identified as *fac* isomers by comparison of their

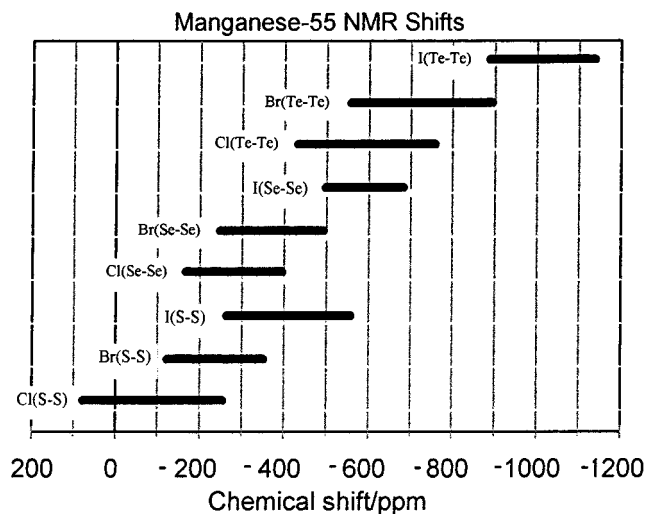


Figure 2. Typical ^{55}Mn chemical shift ranges for $[\text{Mn}(\text{CO})_3\text{X}(\text{L-L})]$ (L-L = dithio-, diseleno-, and ditelluroether).

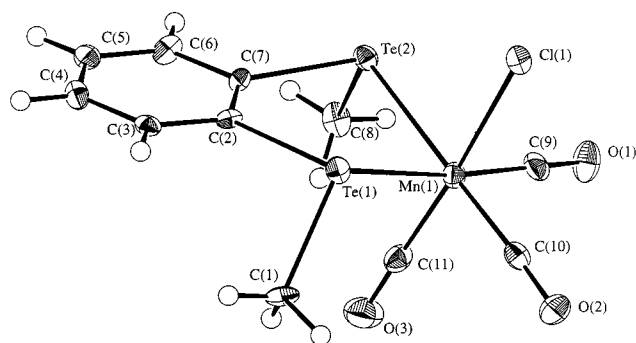


Figure 3. View of the structure of $[\text{Mn}(\text{CO})_3\text{Cl}\{o\text{-C}_6\text{H}_4\text{-(TeMe)}_2\}]$ along with the numbering scheme adopted. Ellipsoids are drawn at the 40% probability level.

IR and NMR spectra (Tables 1 and 2) with the bidentate ligand analogues. However, the product of the reaction of TeMe_2 with $[\text{Mn}(\text{CO})_5\text{Cl}]$ exhibits two closely spaced $\delta(\text{Me})$ resonances in both the ^1H and $^{13}\text{C}\{^1\text{H}\}$ NMR spectra of approximately equal intensity and $\delta(^{125}\text{Te}\{^1\text{H}\})$ resonances at 161 and 271.

The ^{55}Mn spectrum shows a moderately sharp resonance at $\delta - 637$, but on longer accumulations a very broad feature at $\delta - 920$ ($w_{1/2} = 20\,000$ Hz) is seen. A second species is not evident in the carbonyl region of the IR spectrum. This behavior is very similar to that observed in the $[\text{Mn}(\text{CO})_5\text{Cl}]\text{-SbPh}_3$ system,¹⁵ and the second species is identified as the *mer,trans*- $[\text{Mn}(\text{CO})_3\text{Cl}(\text{TeMe})_2]$ isomer, which is also consistent with the much broader ^{55}Mn NMR resonance. In the stibine system,¹⁵ the two $\nu(\text{CO})$ frequencies of the *mer,trans* isomer are at very similar in energy to the two lower bands in the *fac* form, accounting for the difficulty in identifying the second form from the IR spectrum.

X-ray Crystallography. Crystals of $[\text{MnCl}(\text{CO})_3\{o\text{-C}_6\text{H}_4(\text{TeMe})_2\}]$ and $[\text{ReCl}(\text{CO})_3\{o\text{-C}_6\text{H}_4(\text{TeMe})_2\}]$ were obtained from vapor diffusion of petroleum ether into a solution of the complex in CHCl_3 . The compounds are isostructural, showing (Figures 3 and 4, Table 3) a distorted *fac* octahedral geometry with the ditelluroether adopting the *meso-2* arrangement. The Mn-X and

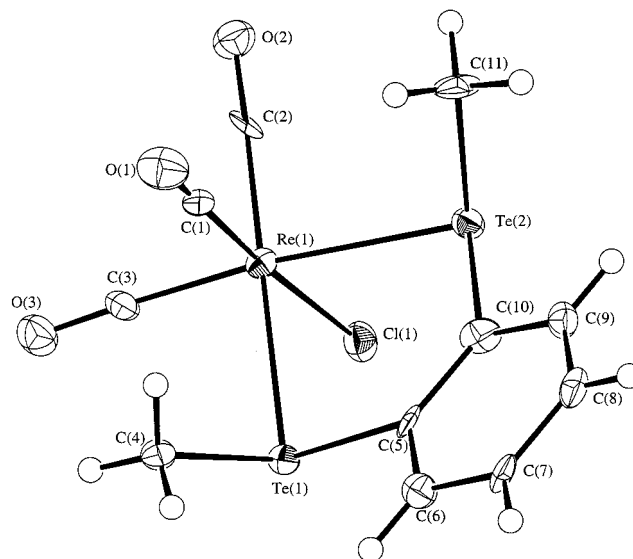


Figure 4. View of the structure of $[\text{Re}(\text{CO})_3\text{Cl}\{o\text{-C}_6\text{H}_4\text{-(TeMe)}_2\}]$ along with the numbering scheme adopted. Ellipsoids are drawn at the 40% probability level.

Table 4. Comparison of NMR Data

complex	$\delta(\text{Se})^a$	$\Delta(\text{Se})^b$	$\delta(\text{Te})^a$	$\Delta(\text{Te})^b$	$\delta(\text{Te})/\delta(\text{Se})$
$[\text{Mn}(\text{CO})_3\text{Cl}\{\text{MeE}(\text{CH}_2)_3\text{EMe}\}]$	91	17	225.5	121.5	2.48
$[\text{Mn}(\text{CO})_3\text{Br}\{\text{MeE}(\text{CH}_2)_3\text{EMe}\}]$	79	5	204.5	100.5	2.59
$[\text{Mn}(\text{CO})_3\text{I}\{\text{MeE}(\text{CH}_2)_3\text{EMe}\}]$	67.5	-6.5	198	94	2.9
$[\text{Mn}(\text{CO})_3\text{Cl}\{o\text{-C}_6\text{H}_4(\text{EMe})_2\}]$	397	195	826.5	454.5	2.08
$[\text{Mn}(\text{CO})_3\text{Br}\{o\text{-C}_6\text{H}_4(\text{EMe})_2\}]$	387	185	817	445	2.11
$[\text{Mn}(\text{CO})_3\text{I}\{o\text{-C}_6\text{H}_4(\text{EMe})_2\}]$	386	184	796	424	2.06
$[\text{Mn}(\text{CO})_3\text{Cl}(\text{EMe})_2]$	66	66	161	161	2.44

^a Averaged chemical shifts from Table 1 and ref 11. ^b $\delta_{\text{complex}} - \delta_{\text{free ligand}}$.

Mn-C distances are very similar to those in analogous thio- and diselenoether complexes,¹¹ while the Mn-E distances (E = S, Se, Te) increase along the series, as would be expected due to the increased radii of E. The structure of $[\text{ReBr}(\text{CO})_3(\text{PhTe}(\text{CH}_2)_3\text{TePh})]$ has been reported by Liaw *et al.*¹⁶

Comparisons. We now compare selected spectroscopic and structural data for $[\text{M}(\text{CO})_3\text{X}(\text{L-L})]$ complexes in an attempt to distinguish the trends in bonding properties of L-L (dithio-, diseleno-, or ditelluroether) in metal carbonyl complexes. Comparisons of structural data for complexes involving Cu^1 , Ag^1 , or Sn^{IV} have shown an increase in M-E of ca. 0.1 Å from E = S to E = Se and a further increase of ca. 0.15 Å to Te.¹⁷ For the $[\text{Mn}(\text{CO})_3\text{X}(\text{L-L})]$ complexes (see ref 11 and the present work), the increase is again about 0.1 Å between Mn-S and Mn-Se. However, the further increase to Mn-Te is only ca. 0.13 Å. A similar difference in $d(\text{Re-Se})$ and $d(\text{Re-Te})$ exists between $[\text{Re}(\text{CO})_3\text{I}(\text{MeSe}(\text{CH}_2)_2\text{SeMe})]$ ¹² and $[\text{Re}(\text{CO})_3\text{Cl}\{o\text{-C}_6\text{H}_4(\text{TeMe})_2\}]$. We must be cautious in interpreting such differences, in that the number of examples is small, and also the data refer in some cases to different chelate ring sizes. However, it is notable that in $[\text{CpFe}(\text{CO})_2(\text{EMe})_2]^+$ the Fe-Te bond length also appears to be shorter than expected, compared with the Fe-S/Fe-Se difference.⁹

(16) Liaw, W.-F.; Horng, Y.-C.; Ou, D.-S.; Chuang, C.-Y.; Lee, C.-K.; Lee, G.-H.; Peng, S.-M. *J. Chin. Chem. Soc. (Taipei)* **1995**, *45*, 59.

(17) Genge, A. R. J.; Levason, W.; Reid, G. *J. Chem. Soc., Dalton Trans.* **1997**, 4549.

(15) Holmes, N. J.; Levason, W.; Webster, M. *J. Organomet. Chem.* **1998**, *568*, 213.

With the caveats noted, the data support the view that the tellurium ligands form shorter and hence stronger bonds to metal carbonyls than would be expected.

We also compared spectroscopic data, specifically the ^{55}Mn , ^{77}Se , and ^{125}Te NMR data and the $\nu(\text{CO})$ vibrations and the derived force constants in the series of $[\text{M}(\text{CO})_3\text{X}(\text{L-L})]$ complexes (Tables 2 and 4). To limit the amount of tabulated data, we have focused on one series of ligands giving six-membered chelate rings $\text{MeE}(\text{CH}_2)_3\text{EMe}$ and the corresponding five-membered chelate ring forming $\sigma\text{-C}_6\text{H}_4(\text{EMe})_2$, although similar trends are present with other ligand types.^{11,12} The ^{55}Mn chemical shifts (Figure 2, Table 1) move progressively to lower frequency as the group 16 donor is changed; $\text{S} \rightarrow \text{Se} \rightarrow \text{Te}$. This increased shielding parallels the decrease in $\nu(\text{CO})$ (below) which is evidence that $\text{L} \rightarrow \text{Mn}$ σ -donation increases in the same direction.¹⁸

For many comparable organoselenium and -tellurium compounds the ^{77}Se and ^{125}Te chemical shifts show very consistent trends and often the $\delta(\text{Te}):\delta(\text{Se})$ ratio is 1.7–1.8 and the $^1J(\text{Te-X}):^1J(\text{Se-X})$ ratio is *ca.* 2–3.¹⁹ We have observed similar trends in Pd(II) and Pt(II) diseleno- and ditelluroether complexes.² Since both Mn and Re are quadrupolar nuclei, no one-bond couplings were resolved. To simplify the comparisons, we have averaged the chemical shifts for the different invertomers of each complex (Table 4). The $\delta(\text{Te}):\delta(\text{Se})$ ratio ranges from 2.1 to 2.9, and although the spread of values suggests that individual values should be treated with some reserve, the overall trend is clear. The ^{125}Te chemical shifts found in the coordinated telluroethers in the present carbonyl complexes are much more positive than expected, either by comparison with the ^{77}Se chemical shifts in the selenoether analogues or by similar comparisons with the same ligands bound to medium-oxidation-state metal centers. Similar conclusions were reached by Schumann and co-workers,¹⁰ from studies of $[\text{CpFe}(\text{CO})(\text{EMe}_2)\text{L}]^+$ ($\text{L} = \text{EMe}_2$ ($\text{E} = \text{S}, \text{Se}, \text{Te}$), PR_3 , AsR_3 , etc.).

The $\nu(\text{CO})$ stretching vibrations are given in Table 2 along with literature data on dithio- and diselenoether complexes. The force constants were obtained *via* the usual secular equations.²⁰ For each complex we have three observed fundamentals, the assignment used being $A'(2) > A'' > A'(1)$, which leads to $K_2 > K_1$ as required^{20,21} and results in sensible values and internally consistent trends in the series. Examination of the data in Table 2 shows that factors such as the halogen present, the chelate ring size, and the R groups on the group 16 donor have some influence, but the most significant trend is with changes in the group 16 donor atom. This is that the CO bonds weaken in the order $\text{S} \rightarrow \text{Se} \rightarrow \text{Te}$, with significantly larger changes between Se and Te than between S and Se. These observations are found for both manganese and rhenium complexes. The rationalization of the trend is that as group 16 is descended more electron density is transferred to the metal, resulting in increased π -acceptance by the car-

Table 5. Crystallographic Data Collection and Refinement Parameters

	$[\text{Mn}(\text{CO})_3\text{Cl}\{\sigma\text{-C}_6\text{H}_4(\text{TeMe})_2\}]$	$[\text{ReCl}(\text{CO})_3\{\sigma\text{-C}_6\text{H}_4(\text{TeMe})_2\}]$
formula	$\text{C}_{11}\text{H}_{10}\text{ClMnO}_3\text{Te}_2$	$\text{C}_{11}\text{H}_{10}\text{ClO}_3\text{ReTe}_2$
fw	535.79	667.06
space group	$P2_1/n$	$P2_1/n$
<i>a</i> , Å	12.721(3)	12.728(6)
<i>b</i> , Å	8.340(6)	8.405(8)
<i>c</i> , Å	13.976(3)	14.095(6)
β , deg	93.16(2)	93.24(4)
<i>V</i> , Å ³	1480(1)	1505(1)
<i>Z</i>	4	4
D_{calcd} , g/cm ³	2.404	2.943
$\mu(\text{Mo K}\alpha)$, cm ⁻¹	49.12	121.70
ψ -scans (max and min transmissn factors)	1.000, 0.852	1.000, 0.593
no. of unique obsd rflns	2798	2847
no. of obsd rflns with $I_0 > 2\sigma(I_0)$	1755	1875
no. of params	163	163
R^a	0.029	0.031
R_w^b	0.029	0.026

$$^a R = \sum(|F_{\text{obs}}| - |F_{\text{c}}|) / \sum |F_{\text{obs}}|. \quad ^b R_w = [\sum w_i(|F_{\text{obs}}| - |F_{\text{c}}|)^2 / \sum w_i |F_{\text{obs}}|^2]^{1/2}.$$

bonyl groups. In metal halide systems, there is some evidence for stronger binding by Se over S, but tellurium ligands appear to bond more weakly as the metal oxidation state increases,⁸ probably due to poor overlap between the large Te σ -donor orbital and the contracted metal orbitals. However, low-valent carbonyl systems, where mismatch of the Te orbitals with the expanded metal orbitals is less likely to be significant, show very good donation from Te and an anomalously large increase from Se to Te.

Experimental Section

Physical measurements were made as described elsewhere.¹¹ One representative example of a complex of each metal is described here. Full details of the syntheses, analytical data, ^1H and $^{13}\text{C}\{^1\text{H}\}$ NMR data, and FAB mass spectra are given in the Supporting Information. All preparations were conducted in dried solvents under a dinitrogen atmosphere. The manganese complexes were stored in foil-wrapped ampules in a refrigerator.

fac $[\text{Mn}(\text{CO})_3\text{Cl}\{\sigma\text{-C}_6\text{H}_4(\text{TeMe})_2\}]$. To a solution of the ditelluroether (0.094 g, 0.26 mmol) in CHCl_3 (40 cm³) was added $[\text{Mn}(\text{CO})_5\text{Cl}]$ (0.06 g, 0.26 mmol) and the solution stirred at room temperature. The progress of the reaction was monitored by removing aliquots of the solution and recording their IR spectra. After 16 h the carbonyl bands of $[\text{Mn}(\text{CO})_5\text{Cl}]$ had been replaced by three new vibrations. The solution was concentrated under vacuum to *ca.* 2 cm³ and cooled in an ice bath, and cold petroleum ether (40–60 °C; 10 cm³) was added to precipitate the yellow product. The precipitate was filtered off, rinsed with cold petroleum ether (1 cm³), and dried *in vacuo*. Yield: 0.111 g, 80%.

fac $[\text{Re}(\text{CO})_3\text{Cl}\{\sigma\text{-C}_6\text{H}_4(\text{TeMe})_2\}]$. A solution of the ditelluroether (0.109 g, 0.30 mmol) in CHCl_3 (40 cm³) and $[\text{Re}(\text{CO})_5\text{Cl}]$ (0.110 g, 0.30 mmol) were refluxed together for 24 h. The progress of the reaction was monitored by removing aliquots of the solution and recording their IR spectra. The solution was worked up as for the manganese analogue to yield a pale orange product. Yield: 0.13 g, 65%.

X-ray Structures of $[\text{Mn}(\text{CO})_3\text{Cl}\{\sigma\text{-C}_6\text{H}_4(\text{TeMe})_2\}]$ and $[\text{Re}(\text{CO})_3\text{Cl}\{\sigma\text{-C}_6\text{H}_4(\text{TeMe})_2\}]$. Details of the crystallographic data collection and refinement parameters are given in Table 5. The crystals were grown by vapor diffusion of petroleum ether (40–60 °C) into solutions of the complexes in CHCl_3 . Data collection used a Rigaku AFC7S four-circle diffractometer

(18) Onaka, S.; Miyamoto, T.; Sasaki, Y. *Bull. Chem. Soc. Jpn.* **1971**, *44*, 1851.

(19) Luthra, N. P.; Odom, J. D. In *The Chemistry of Organic Selenium and Tellurium Compounds*; Patai, S., Rappoport, Z., Eds.; Wiley: New York, 1986; Vol. 1, Chapter 6.

(20) Cotton, F. A. *Inorg. Chem.* **1964**, *3*, 702.

(21) Dalton, J.; Paul, I.; Smith, J. G.; Stone, F. G. A. *J. Chem. Soc. A* **1968**, 1208.

operating at 150 K, using graphite-monochromated Mo K α X-radiation ($\lambda = 0.710\ 73\ \text{\AA}$). Structure solution and refinement were routine.^{22,23}

Additional material available from the Cambridge Crystallographic Data Centre comprises H-atom coordinates, anisotropic thermal parameters, and full listings of bond lengths and angles for the structures.

(22) Beurskens, P. T.; Admiraal, G.; Beurskens, G.; Bosman, W. P.; Garcia-Granda, S.; Gould, R. O.; Smits, J. M. M.; Smykalla, C. PATTY, The DIRDIF Program System; Technical Report of the Crystallography Laboratory; University of Nijmegen: Nijmegen, The Netherlands, 1992.

(23) TeXsan: Crystal Structure Analysis Package; Molecular Structure Corp., The Woodlands, TX, 1995.

Acknowledgment. We thank the EPSRC for support. We also thank Dr. J. S. Ogden for helpful discussions.

Supporting Information Available: Text giving full details of the synthesis of the complexes and analytical and ^1H and $^{13}\text{C}\{^1\text{H}\}$ NMR data. This material is available free of charge via the Internet at <http://pubs.acs.org>.

OM980867U